

the total uterus tissues of the three groups of mice by bisulfite sequencing (Fig. 2A–C). There were 15 CpG sites spanning –272 to +199 of the promoter and the 5'-UTR (exon 1) region of SF-1. The percentages of total methylated CpG sites in this region, in control, and low and high-dose GEN, were 78.3%, 73.9%, and 54.4%, respectively, indicating that GEN dose-dependently induced demethylation in this region. Most CpG sites in the 5'-UTR (exon1) were demethylated by high-dose GEN. In particular, the methylation levels of 5 CpG sites between +45 and +89 were significantly lower in high-dose GEN than in control (Fisher's exact test, $P < 0.01$). We further split the endometrium to separate the luminal side (LU) from the basilar myometrial side (MY), and both specimens were separately subjected to bisulfite sequencing. This procedure was applied to the samples from the GEN-treated groups but not to control samples due to uterus atrophy. In low-dose GEN treated mice, the mean methylation levels of LU and MY were 84.8% and 65.0%, respectively (not shown). In high-dose GEN treated mice, the mean methylation levels of LU and MY were 42.1% and 66.7%, respectively (Fig. 2D). Thus, the demethylation induced by high-dose GEN occurred predominantly in the LU, rather than in the MY.

3.2. Effect of genistein on primary endometrial cell culture

In order to study the SF-1 promoter methylation at the cellular level, we employed an endometrial cell primary culture. Intact

murine endometrium were divided into LU and MY portions, and cells were separately isolated. Primary cell clones were established by colony-formation, following the plating of a serially-titrated cell suspension (see Section 2). Efficient isolated colony formation was achieved with cells seeded at a density of 4,500–15,300 cells/cm². For LU and MY, the average frequencies of colony appearance were 7.5 per 10⁵ cells and 15 per 10⁵ cells, respectively. The growth curves of representative clones derived from LU and MY are shown in Fig. 3. Cell clones with highest and lowest proliferative activities were obtained from LU and MY, separately. More highly proliferative cells were obtained from MY than from LU (Fig. 3A and C). We selected 20 highly proliferative clones for further study (see Section 2). Two rapid growing clones obtained from MY showed self-renewal activity when secondarily seeded at a very low cell density (10 cells/cm²) (not shown). To screen for primary cultured cells that responded to GEN, we set up a high-resolution melting (HRM) assay that identified region-specific methylation levels. The region analyzed by HRM assay exclusively contained the 7 CpG sites between +19 and +89 bp that were most differentially demethylated following oral administration of GEN (Fig. 2). Each clone was treated with or without GEN for 1 week; cells treated with a similar concentration of DMSO served as control. Among the 20 clones that we screened, only one GEN-treated clone (No. 16) exhibited a significant shift in the melting curve compared to control cells (Fig. 4A). This clone had the highest proliferation

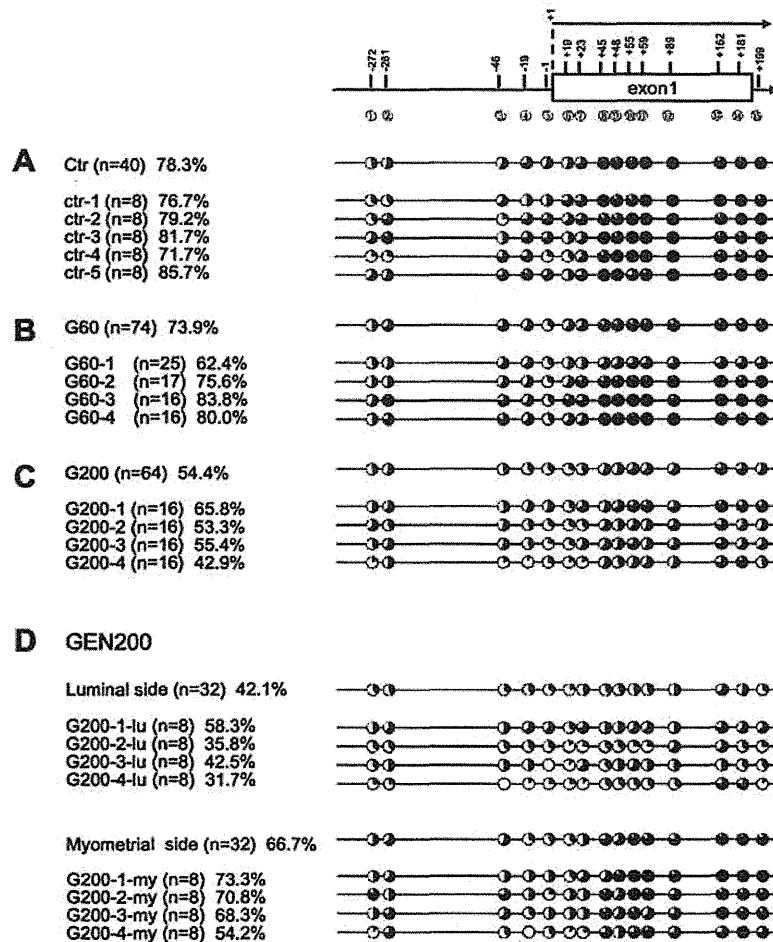


Fig. 2. Genistein induced demethylation of the SF-1 gene promoter in endometrial tissues of OVX mice. The schematic diagram indicates CpG locations on the SF-1 promoter region, spanning 5'-flanking to exon 1. The CpG position relative to the first base of exon 1 (+1) is shown. The bisulfite sequencing fragment contains 15 CpG sites. The black inlay represents the mean methylation levels of each CpG, and the left panel contains the number of sequenced clones and the mean methylation level of all CpGs. Summarized methylation results are shown at the top. (A–C) Difference in methylation levels between (A) vehicle (control), (B) low-dose GEN (60 mg/kg/d), and (C) high-dose GEN (200 mg/kg/d) exposed uteri. (D) Difference in methylation levels between luminal and myometrial sides of a uterus exposed to high-dose GEN.

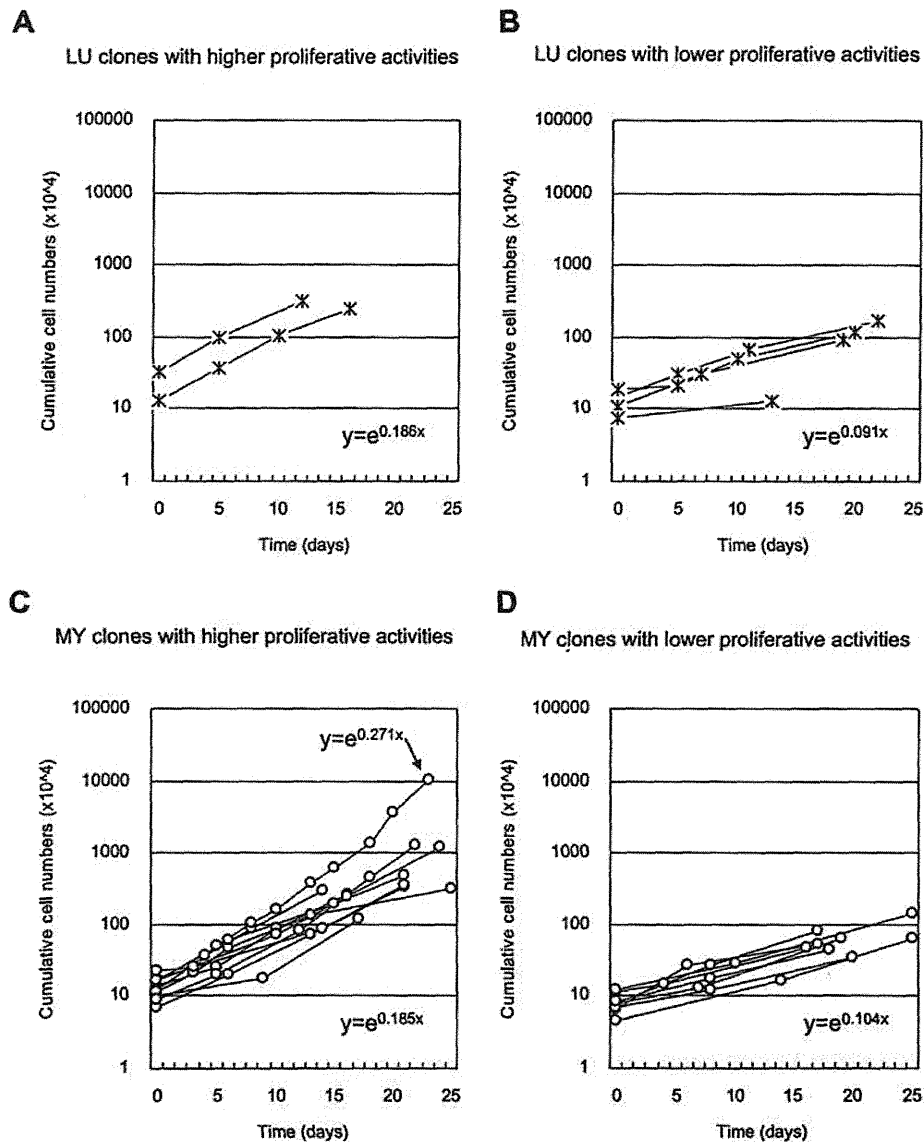


Fig. 3. Proliferation properties of isolated clones: one clone showed highly proliferative activity. Representative growth curves of clones harvested from intact murine endometrium are shown. Formula indicates the slope of fitted growth curves. Clones were divided into two groups: high and low proliferative (see Section 2). A total of 20 highly proliferative clones were analyzed by HRM after *in vitro* GEN treatment. (A, B) Asterisks indicate representative growth curves of cell clones isolated from luminal side. (A) Clones with higher proliferative activities, derived from luminal side. Six highly proliferative clones were obtained in total; 2 representatives are shown. (B) Clones with lower proliferative activities, derived from luminal side. (C, D) Each circle indicates representative growth curves of cell clones isolated from myometrial side. (C) Clones with higher proliferative activities, derived from the myometrial side. In total, 14 highly proliferative clones were obtained; 10 representatives are shown. The arrow indicates the clone with the most rapid growth. (D) Clones with lower proliferative activities, derived from myometrial side.

activity (Fig. 3C, arrow). GEN treatment of the other clones did not result in significant changes to the melting curve patterns (not shown). We further confirmed the methylation status of clone No. 16 by bisulfite sequencing. The percentages of CpG methylation in the SF-1-272 to +199 promoter regions for untreated and GEN-treated cells were 85.0% and 65.8%, respectively (Fig. 4B).

4. Discussion

Growing evidence suggests that the manner in which nutrients can either help maintain health, or conversely, promote disease development may be mediated by epigenetic regulation [12,20]. However, relatively little is known about tissue-specific sensitivity or how much plasticity exists in regards to the effect that a given environmental factor can exert on a certain epigenetic target

[20,21]. GEN, a non-nutrient dietary component of soy products, exhibits mixed estrogen agonist and antagonist properties, and multiple functions both *in vivo* and *in vitro* [7,22]. Several animal studies have demonstrated that GEN acts as an epigenetic modulator [20]. We focused on the effects of GEN on endometrium, because endometrium is not only hormone responsive, but also a highly proliferative organ. Epigenetic alterations of proliferative tissue or cells may then be expanded through tissue proliferation. We used OVX rodents, which are a widely used model for studying estrogen withdrawal and replacement [23], as well as for the assessment of endocrine-disrupting chemicals in the environment [4]. In our experiment, GEN induced proliferation of the endometrium and increased uterine weight (Fig. 1A) to extents similar to those previously reported in OVX rats [4]. Our findings also suggested that GEN treatment induced marked demethylation of

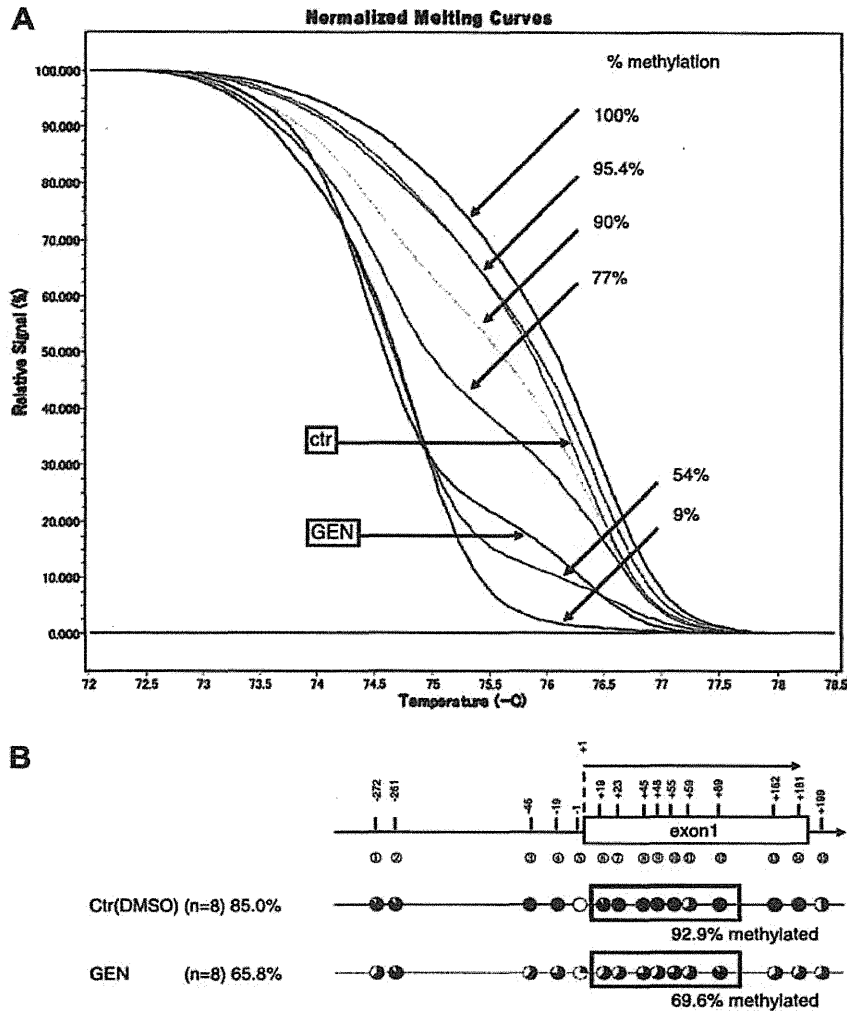


Fig. 4. Genistein induced demethylation of the SF-1 gene in the cell clone that showed the highest proliferative activity. (A) The GEN-mediated demethylation of CpGs (at the positions of +19, 23, 45, 48, 55, 59, and 89) in the SF-1 gene *in vitro* in one out of 20 isolated clones (Fig. 3A and C). HRM analysis enabled to clear separation of the PCR product mixtures with different CpG compositions. The methylation standards were prepared as 100% (red), 95.4% (orange), 90% (yellow), 77% (green), 54% (blue), and 9% (violet) methylated template in demethylated background. Grey and pink indicate the control and GEN-treated clone sample, respectively. (B) SF-1 DNA methylation status, obtained from bisulfate sequencing, of the clone that showed demethylation in HRM assay. Percentage under box (HRM region) indicates percent methylation of HRM region. (For interpretation of the references to color in this figure legend, the reader is referred to the web version of this paper.)

CpG sites in the SF-1 promoter (Fig. 2), and substantial increase in SF-1 mRNA level (Fig. 1B). Expressions of genes downstream of transcription factor SF-1 were also significantly enhanced (Fig. 1C–F). However, it should be noted that the induced mRNA levels were still very low (Fig. 1B–F), less than one copy per cell, as determined by the Percellome method [16]. Our results are consistent with those of a previous study reporting that a physiological concentration of GEN increased Cyp19a1 enzymatic activity in endometrial cells derived from a normal uterus, whereas GEN did not affect Cyp19a1 activity in a cell-free assay [24]. It is unknown whether GEN stimulated Cyp19a1 activity by epigenetic modulation.

In the present study, we also identified primary cultured endometrial cells that were competent for epigenetic regulation by GEN, which were present at a very low frequency. In our *in vitro* study, GEN treatment did not enhance, but rather inhibited the proliferation of colony-derived cells. Taken together, these findings indicate that a minor population of endometrium cells can respond to GEN and that, in these cells, GEN induces demethylation and

activation of SF-1, followed by the induction of the SF-1 steroidogenic cascade. This might lead to local steroidogenesis and enhanced endometrium proliferation *in vivo* in GEN-treated OVX mice. Since demethylation of the SF-1 promoter was observed at the whole tissue level (Fig. 2), and the induced expression of steroidogenic genes occurred only to a subcellular amount (Fig. 1B–F), the demethylation event in each cell may not be sufficient for the SF-1 induction.

The demethylation in the endometrium that occurred after 1 week of treatment with high-dose GEN was more prominent in the LU than in the MY. Following GEN treatment, the methylation level in the MY was similar to that in the untreated endometrium as a whole. After 7 days of GEN exposure, the endometrial cells in the LU of OVX mice were composed of regenerated cells moving from MY to LU; in light of this, our results indicate that the initial epigenetic alteration might be expanded through proliferation of regenerating cells. This is also consistent with our observation that more endometrial cells derived from MY showed higher colony-formation activity and rapid proliferation than did those derived

from LU (Fig. 3). We thus speculate that there are GEN-sensitive cells in the MY, which might contain endometrial stem cells [25].

Recently, human endometrial stem cells were identified; they reside in endometrial stromal tissue and possess fibroblastic-shape and self-renewal ability, thus forming large, densely packed, homogenous colonies [17,18]. Some candidates for murine endometrial progenitor cells have been suggested to reside in the luminal epithelial or area of adjacent to the myometrium [25]. The rapidly growing endometrial cell that we obtained had a fibroblastic-shape, formed large, relatively homogenous, densely packed colonies, and showed self-renewal activity when seeded at a very low cell density (data not shown). Although there are differences between the species, we speculate that our rapid growing cell clones may correspond to the human endometrial stromal progenitor cells [17].

Aberrant SF-1 expression with lack of promoter CpG methylation has been reported in ectopic endometriosis [14], and thus endometriosis is now considered an epigenetic disease [26]. Endometriosis is classically defined as the growth of endometrial tissue at extrauterine sites; it has been suggested that each endometriotic lesion originates from a single epigenetically deregulated endometrial progenitor cell [27]. Further studies are required to identify cells which are competent for epigenetic changes following GEN exposure, and to elucidate the relationships between these cells, GEN, and endometriosis.

In conclusion, we demonstrated that GEN demethylates the promoter region of the SF-1 gene. This is the first demonstration of phytoestrogen participation in epigenetic alterations in adult endometrial tissue. These findings are important from standpoints of nutrition, public health, and disease prevention. Further study is warranted to characterize the nature of the cells that respond to GEN in the endometrium.

Appendix A. Supplementary data

Supplementary data associated with this article can be found, in the online version, at doi:10.1016/j.bbrc.2011.07.104.

References

- [1] H. Adlercreutz, Phyto-estrogens and cancer, *Lancet Oncol.* 3 (2002) 364–373.
- [2] M. Messina, W. McCaskill-Stevens, J.W. Lampe, Addressing the soy and breast cancer relationship: review, commentary, and workshop proceedings, *J. Natl. Cancer Inst.* 98 (2006) 1275–1284.
- [3] A.H. Wu, R.G. Ziegler, A.M. Nomura, D.W. West, L.N. Kolonel, P.L. Horn-Ross, R.N. Hoover, M.C. Pike, Soy intake and risk of breast cancer in Asians and Asian Americans, *Am. J. Clin. Nutr.* 68 (1998) 1437S–1443S.
- [4] J. Kanno, L. Onyon, S. Peddada, J. Ashby, E. Jacob, W. Owens, The OECD program to validate the rat uterotrophic bioassay. Phase 2: dose–response studies, *Environ. Health Perspect.* 111 (2003) 1530–1549.
- [5] K. Pettersson, J.A. Gustafsson, Role of estrogen receptor beta in estrogen action, *Annu. Rev. Physiol.* 63 (2001) 165–192.
- [6] P. Diel, T. Hertrampf, J. Seibel, U. Laudenschlager, S. Kolba, G. Vollmer, Combinatorial effects of the phytoestrogen genistein and of estradiol in uterus and liver of female Wistar rats, *J. Steroid Biochem. Mol. Biol.* 102 (2006) 60–70.
- [7] V. Beck, U. Rohr, A. Jungbauer, Phytoestrogens derived from red clover: an alternative to estrogen replacement therapy?, *J. Steroid Biochem. Mol. Biol.* 94 (2005) 499–518.
- [8] N. Sato, N. Yamakawa, M. Masuda, K. Sudo, I. Hatada, M. Muramatsu, Genome-wide DNA methylation analysis reveals phytoestrogen modification of promoter methylation patterns during embryonic stem cell differentiation, *PLoS One* 6 (2011) e19278.
- [9] S.M. Meeran, A. Ahmed, T.O. Tollefsbol, Epigenetic targets of bioactive dietary components for cancer prevention and therapy, *Clin. Epigenetics* 1 (2010) 101–116.
- [10] S. Majid, A.A. Dar, V. Shahryari, H. Hirata, A. Ahmad, S. Saini, Y. Tanaka, A.V. Dahiya, R. Dahiya, Genistein reverses hypermethylation and induces active histone modifications in tumor suppressor gene B-Cell translocation gene 3 in prostate cancer, *Cancer* 116 (2010) 66–76.
- [11] A.K. Jha, M. Nikbakht, G. Parashar, A. Shrivastava, N. Capalash, J. Kaur, Reversal of hypermethylation and reactivation of the RARbeta2 gene by natural compounds in cervical cancer cell lines, *Folia. Biol. (Praha)* 56 (2010) 195–200.
- [12] Y. Li, T.O. Tollefsbol, Impact on DNA methylation in cancer prevention and therapy by bioactive dietary components, *Curr. Med. Chem.* 17 (2010) 2141–2151.
- [13] K. Morohashi, S. Honda, Y. Inomata, H. Handa, T. Omura, A common trans-acting factor, Ad4-binding protein, to the promoters of steroidogenic P-450s, *J. Biol. Chem.* 267 (1992) 17913–17919.
- [14] Q. Xue, Z. Lin, P. Yin, M.P. Milad, Y.H. Cheng, E. Confino, S. Reierstad, S.E. Bulun, Transcriptional activation of steroidogenic factor-1 by hypomethylation of the 5' CpG island in endometriosis, *J. Clin. Endocrinol. Metab.* 92 (2007) 3261–3267.
- [15] S.E. Bulun, H. Utsunomiya, Z. Lin, P. Yin, Y.H. Cheng, M.E. Pavone, H. Tokunaga, E. Trukhacheva, E. Attar, B. Gurates, M.P. Milad, E. Confino, E. Su, S. Reierstad, Q. Xue, Steroidogenic factor-1 and endometriosis, *Mol. Cell. Endocrinol.* 300 (2009) 104–108.
- [16] J. Kanno, K. Aisaki, K. Igarashi, N. Nakatsu, A. Ono, Y. Kodama, T. Nagao, "Per cell" normalization method for mRNA measurement by quantitative PCR and microarrays, *BMC Genomics* 7 (2006) 64.
- [17] R.W. Chan, K.E. Schwab, C.E. Gargett, Clonogenicity of human endometrial epithelial and stromal cells, *Biol. Reprod.* 70 (2004) 1738–1750.
- [18] C.E. Gargett, K.E. Schwab, R.M. Zillwood, H.P. Nguyen, D. Wu, Isolation and culture of epithelial progenitors and mesenchymal stem cells from human endometrium, *Biol. Reprod.* 80 (2009) 1136–1145.
- [19] Y. Kumaki, M. Oda, M. Okano, QUMA: quantification tool for methylation analysis, *Nucleic Acids Res.* 36 (2008) W170–W175.
- [20] J.A. McKay, J.C. Mathers, Diet induced epigenetic changes and their implications for health, *Acta Physiol. (Oxf)* (2011) 103–118.
- [21] B.C. Christensen, E.A. Houseman, C.J. Marsit, S. Zheng, M.R. Wrensch, J.L. Wiemels, H.H. Nelson, M.R. Karagas, J.F. Padbury, R. Bueno, D.J. Sugarbaker, R.F. Yeh, J.K. Wiencke, K.T. Kelsey, Aging and environmental exposures alter tissue-specific DNA methylation dependent upon CpG island context, *PLoS Genet.* 5 (2009) e1000602.
- [22] C.B. Klein, A.A. King, Genistein genotoxicity: critical considerations of in vitro exposure dose, *Toxicol. Appl. Pharmacol.* 224 (2007) 1–11.
- [23] G. Rimoldi, J. Christoffel, D. Seidlova-Wuttke, H. Jarry, W. Wuttke, Effects of chronic genistein treatment in mammary gland, uterus, and vagina, *Environ. Health Perspect.* 115 (Suppl. 1) (2007) 62–68.
- [24] K.M. Edmunds, A.C. Holloway, D.J. Crankshaw, S.K. Agarwal, W.G. Foster, The effects of dietary phytoestrogens on aromatase activity in human endometrial stromal cells, *Reprod. Nutr. Dev.* 45 (2005) 709–720.
- [25] C.E. Gargett, H. Masuda, Adult stem cells in the endometrium, *Mol. Hum. Reprod.* 16 (2010) 818–834.
- [26] S.W. Guo, Epigenetics of endometriosis, *Mol. Hum. Reprod.* 15 (2009) 587–607.
- [27] Y. Wu, Z. Basir, A. Kajdacsy-Balla, E. Strawn, V. Macias, K. Montgomery, S.W. Guo, Resolution of clonal origins for endometriotic lesions using laser capture microdissection and the human androgen receptor (HUMARA) assay, *Fertil. Steril.* 79 (Suppl. 1) (2003) 710–717.

Endocrine disrupter bisphenol A increases *in situ* estrogen production in mouse urogenital sinus

BPA increases estrogen production

Shigeki Arase^{1,4}, Kenichiro Ishii^{1,4,5}, Katsuhide Igarashi², Kenichi Aisaki², Yuko Yoshio¹, Ayami Matsushima³, Yasuyuki Shimohigashi³, Kiminobu Arima¹, Jun Kanno², Yoshiki Sugimura^{1,*}

¹ Department of Nephro-Urologic Surgery and Andrology, Mie University Graduate School of Medicine, Mie, Japan

² Division of Cellular & Molecular Toxicology, National Institute of Health Sciences, Tokyo, Japan

³ Laboratory of Structure-Function Biochemistry, Department of Chemistry, Faculty of Sciences, Kyushu University, Fukuoka, Japan

* Correspondence to: Department of Nephro-Urologic Surgery and Andrology, Mie University Graduate School of Medicine, 2-174 Edobashi, Tsu, Mie 514-8507, Japan. Tel: +81-59-231-5026, Fax: +81-59-231-5203

E-mail: sugimura@clin.medic.mie-u.ac.jp

⁴ The first two authors contributed equally to this work.

⁵ Current address: Mie University Graduate School of Regional Innovation Studies, 1577 kurimamachiya-cho, Tsu, Mie 514-8507, JAPAN

Keywords: Bisphenol A; Urogenital sinus; *In situ* estrogen production; Aromatase; Steroidogenic enzyme

Abbreviations: EDC, endocrine-disrupting chemical; BPA, bisphenol A; DES, diethylstilbestrol; E₂, estradiol; UGS, urogenital sinus; UGE, urogenital sinus epithelium; UGM, urogenital sinus mesenchyme; Ad4BP/SF-1, adrenal-4 binding protein/steroidogenic factor-1; ERR γ , estrogen-related receptor γ .

Disclosure Summary: The authors have nothing to disclose.

Grant support: This study was supported by Grants-in Aid from the Ministry of Health, Labor and Welfare, Japan.

GEO accession number: GSE24928

ABSTRACT

The balance between androgens and estrogens is very important in the development of the prostate, and even small changes in estrogen levels, including those of estrogen-mimicking chemicals, can lead to serious changes. Bisphenol A (BPA), an endocrine-disrupting chemical (EDC), is a well-known, ubiquitous estrogenic chemical. To investigate the effects of fetal exposure to low-dose BPA on the development of the prostate, we examined the alterations of *in situ* sex steroid hormonal environment in the mouse urogenital sinus (UGS). In the BPA-treated UGS, E₂ levels and aromatase activity were significantly increased as compared with the untreated and DES-treated UGS. The mRNAs of steroidogenic enzymes, *Cyp19a1* and *Cyp11a1*, and sex-determining gene *Nr5a1* were up-regulated specifically in the BPA-treated group. The up-regulations of mRNAs were observed in the mesenchymal component of UGS (urogenital sinus mesenchyme; UGM), as well as in the cerebellum, heart, kidney, and ovary but not in the testis. The number of aromatase-expressing mesenchymal cells in the BPA-treated UGS was approximately twice compared to that in the untreated and DES-treated UGS. The up-regulation of *Esrrg* mRNA was observed in organs for which mRNAs of steroidogenic enzyme were also up-regulated. We demonstrated here that fetal exposure to low-dose BPA had the unique action which was the increases of *in situ* E₂ levels and CYP19A1 (aromatase) activity in the mouse UGS. Our data suggest that BPA might interact with *in situ* steroidogenesis by altering tissue components, such as the accumulation of aromatase-expressing mesenchymal cells, in particular organs.

INTRODUCTION

Endocrine-disrupting chemicals (EDCs) have been implicated to alter the fetal development of urogenital organs as well as the reproductive and endocrine systems in humans and other species [1]. The fetal development of urogenital organs is induced by endogenous hormonal messages that originate in fetal and maternal hormone systems. Fetal exposure to EDCs disrupts the interactions between endogenous hormones and their receptors, causing adverse effects later in life [2]. In the prostate, both androgens and estrogens play a significant role in development and differentiation as well as the maintenance of adult homeostasis [3]. Therefore, even small changes in estrogen levels, including estrogen-mimicking chemicals, can lead to changes in prostate development and differentiation.

Bisphenol A (BPA), one of the EDCs, is a well-known, ubiquitous estrogenic chemical used in the manufacture of polycarbonate plastics, as a lining in metal food and drink cans, and as dental sealants [4]. The concern with BPA originates from its detection in maternal and fetal plasma as well as the placenta [5] [6]. Thus, fetal exposure to BPA is implicated in fetal toxicity, as well as in subsequent growth of the infant. Histopathologically, fetal exposure to low-dose BPA (10 µg/kg/day) has been shown to increase cell proliferation of urogenital sinus epithelium (UGE) in the primary prostatic ducts of CD1 mice [7]. Recently, our group reported that fetal exposure to low-dose BPA (20 µg/kg/day) specifically increased the number of basal epithelial cells in the adult prostate of BALB/c mice, and also induced permanent cytokeratin 10 (KRT10) expression in such cells similar to the effects of synthetic estrogen diethylstilbestrol (DES, 0.2 µg/kg/day) [8]. Epigenetically, neonatal exposure of male rats to low-dose BPA (10 µg/kg/day) elicited critical molecular changes during prostate development and also increased prostatic gland susceptibility to precancerous neoplastic lesions and hormonal carcinogenesis [9]. Below 50 µg/kg/day, toxicological studies of BPA in rodent fetuses and offspring have demonstrated alterations of mammary gland development, open-field behavior, and reproductive functioning [10] [11] [12].

Some EDCs are reported to alter the *in situ* sex steroid hormonal environment in the reproductive system. The triazine herbicide atrazine binds directly to adrenal-4 binding protein/steroidogenic factor-1 (Ad4BP/SF-1, official symbol NR5A1) and increases CYP19A1 (aromatase) expression and ultimately estradiol (E₂) production in human genital cancer cell lines [13]. The aryl hydrocarbon (dioxin) also increases CYP19A1 (aromatase) expression mediated by its receptor in mouse ovaries [14]. In contrast, the phosphorothioate insecticide profenofos increases the expression of steroidogenic genes and testosterone (T) levels in rat testes [15]. Recently reported adverse effects of BPA on *in situ* steroidogenesis included increased T levels in mouse Leydig cells and decreased E₂ levels in porcine ovarian granulosa cells [16] [17]. Thus, BPA may have the potential to not only mimic estrogenic action but also alter *in situ* steroidogenesis in the prostate as well as other reproductive organs.

To investigate the effects of fetal exposure to low-dose BPA on *in situ* steroidogenesis in the developing prostate, we first measured sex steroid hormone levels and CYP19A1 (aromatase) activity in the BPA-treated mouse urogenital sinus (UGS), from which prostate develops embryologically. Subsequently, we examined the alterations of steroidogenic enzyme gene expression to confirm the alterations of the *in situ* sex steroid hormonal environment in the BPA-treated mouse UGS. Finally, we identified the BPA-specific biological effects for *in situ* steroidogenesis during fetal prostate development.

MATERIALS AND METHODS

Animals

Three female C57BL/6 mice (10 weeks of age) were mated with one male overnight, and then they were separated next morning (plug date denoted as day 0). In this study, 36 pregnant female C57BL/6 mice were purchased on the 12th day of gestation from Japan SLC (Shizuoka, Japan). All animals were housed individually in chip-bedded polyolefin cages in a room with controlled temperature (23 ± 1°C) and humidity (45 ± 65%) on a 12/12-h light/dark cycle. Mice were fed a phytoestrogen-low diet (NIH-07PLD; Oriental Yeast Co., Tokyo, Japan) and tap water *ad libitum*.

Chemicals

BPA and DES with a purity of $\geq 99\%$ were purchased from Nacalai Tesque (Kyoto, Japan) and Wako Pure Chemical Industries (Osaka, Japan), respectively.

Fetal exposure to chemicals

We randomly assigned 36 pregnant female C57BL/6 mice to three different treatment groups: i.e., BPA (20 $\mu\text{g}/\text{kg}/\text{day}$, $n = 12$) or DES (0.2 $\mu\text{g}/\text{kg}/\text{day}$, $n = 12$), which were dissolved in tocopherol-stripped corn oil (MP Biomedical Inc., Solon, OH, USA) by oral gavages, on embryonic day 13 (E13) to E16. For the control group, pregnant mice were fed tocopherol-stripped corn oil (2 ml/kg) ($n = 12$). Previously, our group reported that this protocol of fetal exposure to BPA and DES resulted in similar histopathological changes in adult prostate: i.e., increase of basal epithelial cell number and induction of cytokeratin 10 (KRT10), a classic marker associated with squamous differentiation, in such cells [8]. Our dose level of BPA was also based on reported results suggesting that BPA is < 100 -fold less potent than DES. The Mie University's Committee on Animal Investigation approved the experimental protocol.

Termination and UGS dissection

Between E17 and postnatal day 1 (P1), all animals were terminated by an overdose of isoflurane followed by cervical dislocation. For each group, $n = 15\sim 18$ fetuses (for both male and female) from 3 pregnant mice were collected at E17, E18, P0, and P1. The bladder and urethra were removed and dissected to isolate UGS, and then the 5~6 UGSs were pooled as 1 sample. Thus, the 15~18 UGSs were divided into 3 samples at each time point. The UGS, cerebellum, heart, kidney, testis, and ovary were collected in RNA *later* (Applied Biosystems, Foster City, CA, USA).

To isolate pure UGS, other tissues such as the bladder, urethra, Wolffian duct (WD), seminal vesicle (SV), and Mullerian duct (MD) were removed from both the male and female urogenital tracts. The histopathology of the mouse UGS was then examined by hematoxylin and eosin staining.

Measurements of in situ E_2 levels and CYP19A1 (aromatase) activity in UGS

E_2 levels and CYP19A1 (aromatase) activity in UGS were determined by liquid chromatography-tandem mass spectrometry (LC-MS/MS) [18] and a tritiated water release assay [19], respectively, which were made available by Aska Pharma Medical (Kanagawa, Japan). Briefly, the organs were homogenized, and the extracts were applied to a C18 Amprep solid-phase column (Amersham Biosciences, Arlington Heights, IL, USA) to remove contaminating fats. E_2 was then separated using a normal-phase high-performance liquid chromatography (HPLC) system (Jasco, Tokyo, Japan) with a silica gel column (Cosmosil 5SI; Nacalai Tesque, Kyoto, Japan), and 100 pg isotope-labeled [$^{13}\text{C}_4$]- E_2 was added to extracts. The evaporated extracts were reacted with 5% pentafluorobenzyl bromide/acetonitrile, under KOH/ethanol, for 1 h at 55°C. After evaporation, the products were reacted with 100 ml picolinic acid solution (2% picolinic acid, 2% 2-dimethylaminopyridine, and 1% 2-methyl-6-nitrobenzoic acid in tetrahydrofuran) and 20 ml triethylamine for 0.5 h at room temperature. The reaction products were dissolved in 1% acetic acid and were purified using a Bond Elute C18 column (Varian, Palo Alto, CA, USA). The products were measured with a reverse-phase LC (Agilent 1100, Agilent Technologies, Santa Clara, CA, USA) coupled with an API 5000 triple-stage quadrupole mass spectrometer (Applied Biosystems, Foster City, CA, USA) in the positive-ion mode. This device monitored the m/z 558 to m/z 339 (E_2) and m/z 562 to m/z 343 ([$^{13}\text{C}_4$]- E_2) transitions.

The tritiated water release assay was used for the measurement of CYP19A1 (aromatase) activity. This method measures the production of $^3\text{H}_2\text{O}$, which forms as a result of aromatization of the substrate [$1\text{b-}^3\text{H}$]-androst-4-ene-3,17-dione (New England Nuclear, Boston, MA, USA). Serum-free medium containing [$1\text{b-}^3\text{H}$]-androst-4-ene-3,17-dione solution (54 nM) was prepared, of which 0.5 ml was added to each sample. After incubation for 1 h, the samples were placed on ice and 200 μl of culture medium was

withdrawn. The medium was extracted with 500 μ l chloroform, vortexed, and then centrifuged for 1 min at 9000 \times g. A 100 μ l aliquot of the aqueous phase was mixed with 100 μ l of a 5% wt/vol charcoal 0.5% wt/vol dextran T-70 suspension, vortexed, and then incubated for 10 min. After centrifugation of the solution for 5 min at 9000 \times g, a 150 μ l aliquot was removed for measurement of radioactivity by liquid scintillation.

RNA extraction and cDNA preparation

Total RNA was extracted using the Qiagen mini RNA Easy kit in accordance with the manufacturer's instructions (Qiagen Inc., Valencia, CA, USA). The RNA concentration was then determined spectrophotometrically by multi-Detection Microplate Reader (Dainippon Sumitomo Pharma Co., Osaka, Japan). From 50 ng of total RNA, cDNA was reverse transcribed using oligo (dT) and Superscript II RNase H-reverse transcriptase (Invitrogen Co., Carlsbad, CA, USA) as previously described [8].

Analysis of gene expression profile

For determining gene expression profiles of the male UGS, GeneChip analysis with the Percellome method was performed [20]. Briefly, organs were prepared using RLT buffer (Qiagen Inc., Valencia, CA, USA). Total RNA was extracted using RNeasy Mini Kit (Qiagen Inc., Valencia, CA, USA). First-strand cDNA was synthesized by incubating 5 mg of total RNA with a T7 oligo (dT) primer (Invitrogen Co., Carlsbad, CA, USA) according to the manufacturer's protocol. The dsDNA was mixed with T7 RNA polymerase (Enzo Biochem., Farmingdale, NY, USA). During the *in vitro* transcription, generated cRNAs were labeled with biotin-16-UTP and biotin-11-CTP (Enzo Biochem., Farmingdale, NY, USA). The purified cRNA was fragmented at 300–500 bp into the target solution. Hybridization was performed with the GeneChip Mouse Genome 430 ver. 2.0 (Affymetrix Inc., Santa Clara, CA, USA) at 45°C for 18 h after staining with streptavidin-R-phycoerythrin conjugates (Molecular Probes, Invitrogen Co., Carlsbad, CA, USA). The reacted arrays were then scanned as digital image files, and the scanned data were analyzed with GeneChip Operating Software (Affymetrix Inc., Santa Clara, CA, USA). The expression data were converted to copy numbers of mRNA per cell by the Percellome method, quality controlled, and analyzed using Percellome software [20].

Real-time polymerase chain reaction (PCR) analysis

Real-time PCR was carried out in the iCycler iQ Detection System (Bio-Rad laboratories, Hercules, CA, USA) with iQ SYBR-Green Supermix reagents (Bio-Rad laboratories, Hercules, CA, USA) as previously described [8]. PCR amplification reaction was performed with specific primers as shown in Table 1. After PCR, melting curve analysis was performed to verify specificity and identity of the PCR products. All data were analyzed with the iCycler iQ Optical System Software Version 3.0A (Bio-Rad laboratories, Hercules, CA, USA). All the PCR data was normalized to *Gapdh* mRNA.

Preparation of primary cultured mesenchymal cells from UGS

UGS were dissected from the fetuses and separated into urogenital sinus epithelial (UGE) and urogenital sinus mesenchymal (UGM) components by tryptic digestion and mechanical separation as previously described [21]. UGM were cultured in RPMI-1640 with 5% FBS and plated out on 4-well glass slides (BD Falcon, Franklin Lakes, NJ USA). After several days, cells were fixed in methanol and processed for immunocytochemical analysis.

Immunocytochemical staining

The sections were first incubated for 15 min in 0.01 M PBS. After inhibition of endogenous peroxidases (10 min in 0.6% H₂O₂ diluted in 0.01 M PBS plus 0.2% Triton X-100, PBST), and saturation (2 h in a 5% normal goat serum solution), they were incubated overnight at 4°C in a polyclonal affinity-purified anti-aromatase antibody or ERR γ antibody raised in rabbit against quail recombinant aromatase or ESRRG diluted 1:500 in 0.01 M PBST. The next day the sections were immersed for 2 h at room temperature in a biotin-conjugated goat anti-rabbit IgG (DakoCytomation, Inc., Copenhagen, Denmark) diluted 1:400 in

PBST and subsequently for 2 h in a streptavidin-fluorescein complex (Rhodamine, DakoCytomation, Inc., Copenhagen, Denmark) diluted 1:50 in PBST. Between each step, sections were extensively rinsed in PBST. The sections were mounted onto microscope slides, coverslipped with a gelatin-based mounting medium, and stored in the dark at 4°C. For double-labeling immunofluorescence, Alexa Fluor 488-conjugated or 594-conjugated secondary antibodies were used. Rabbit polyclonal anti-aromatase antibody was kindly provided by Professor Nobuhiro Harada (Department of Biochemistry, Fujita Health University School of Medicine, Aichi, Japan) [22]. The rabbit polyclonal anti-ESRRG antibody used here was established and characterized as previously reported [23]. The mouse monoclonal anti-Ran antibody (Santa Cruz Biotechnology, Inc., Santa Cruz, CA, USA) was used to detect nucleus in cells. Ran, also called TC4, is the small RAS-related protein which is localized in nucleus.

Statistical analysis

The results were expressed as means \pm S.D. Differences among the three groups were determined using Student's *t*-test with Dunnett multiple comparison. $p < 0.05$ was considered statistically significant.

RESULTS

BPA-specific increases of E₂ levels and CYP19A1 (aromatase) activity in mouse UGS

The pregnant mice were exposed to low-dose BPA during the onset of prostatic budding (E13-E16), and UGS of fetuses was collected during bud elongation (E17-P1). In analyses of *in situ* sex steroid hormonal environment, E₂ levels and CYP19A1 (aromatase) activity were significantly increased only at P1 in BPA-treated UGS but not at P1 in the DES-treated UGS (Figure 1). At E17 and P1, both the E₂ levels and CYP19A1 (aromatase) activity in untreated male UGS were not significantly different compared with untreated female UGS.

BPA-specific up-regulations of steroidogenic enzyme and sex-determining gene mRNA in mouse UGS

To investigate the BPA-specific gene alterations related to increases of the E₂ levels and aromatase activity, we performed preliminarily GeneChip analysis with the Percellome method in the BPA-treated or DES-treated male UGS at E17 and P1. The results showed BPA-specific up-regulations of steroidogenic enzymes, such as *Cyp11a1*, *Cyp11b1*, and *Cyp17a1*, and sex-determining factors, such as *Nr5a1*, *Nr0b1*, *Gata4*, and *Amhr2* (data not shown). Furthermore, quantitative PCR analysis confirmed the mRNA up-regulations of *Cyp19a1*, *Cyp11a1*, and *Nr5a1* only in the BPA-treated neonatal (P0 and P1) UGS but not in the DES-treated neonatal UGS (Figure 2). There was no difference in mRNA expression levels between E17 and P1 when comparing the untreated male UGS to that of the female. In untreated male and female UGS, the mRNA of *Cyp19a1* was gradually increased between E17 and P1.

Restricted BPA-specific up-regulations of steroidogenic enzyme and sex-determining gene mRNA in mesenchymal component of UGS

In male fetuses at P1, it was not feasible to separate UGE and UGM components within the male UGS due to the formation of prostatic buds. In female at P1, the up-regulations of *Cyp19a1*, *Cyp11a1*, and *Nr5a1* mRNA were observed only in UGM but not in UGE of the BPA-treated group (Figure 3). In both the male and female UGE, expressions of such mRNAs were quite low and not up-regulated, even in the BPA-treated group. At E17, there was no difference in mRNA expression levels when comparing the untreated male UGM with that of the female.

BPA-specific increases of aromatase-expressing cells in primary cultured UGM

In both the male and female, P1 UGM was primary cultured *in vitro*. Representative pictures of aromatase-positive cells are shown in Figure 4A–4C. The aromatase-positive staining was observed in the cytoplasm of cultured UGM. The rate of positivity, i.e., percentage of cells that expressed CYP19A1 (aromatase) protein, was approximately 10% in the untreated and the DES-treated groups, whereas it was as high as approximately 30% in the BPA-treated group (Figure 4D). There was no difference in the rate of positivity of CYP19A1 (aromatase) when comparing the untreated male UGM to that of the female.

Restricted BPA-specific up-regulation of Esrrg mRNA in the mesenchymal component of UGS

In E17 female UGM, the mRNA expression of *Esr1* was up-regulated by both BPA and DES treatment (Figure 5A). At E17, however, the mRNA expression of *Ar* was up-regulated by both BPA and DES treatment in the male UGS (Figure 5B). At P1, mRNA expression of *Ar* was up-regulated by both BPA and DES treatment in the female UGS (Figure 5B). In both the male and female, the up-regulation of *Esrrg* mRNA was observed at E17 and restricted in UGM of the BPA-treated group but not in UGE (Figure 5C). In both the male and female UGE, the expression of *Esrrg* mRNA was quite low and not up-regulated, even in the BPA-treated group. At E17, there was no difference in mRNA expression levels when comparing the untreated male UGS with that of the female.

BPA-specific increases of ESRRG-expressing cells in primary cultured UGM

In both the male and female, E17 UGM was primary cultured *in vitro*. Representative pictures of ESRRG-positive cells are shown in Figures 6A–6C. The ESRRG-positive staining was observed in both the nucleus and the cytoplasm of cultured UGM. The number of ESRRG-positive UGM was significantly increased only in the BPA-treated group and showed a 2.2-fold increase in males and a 1.6-fold increase in females (Figure 6D). There was no difference in the rate of positivity of ERR γ when comparing the untreated male UGM with that of the female.

BPA-specific up-regulations of Esrrg and steroidogenic enzyme mRNA in sex hormone-related organs

To investigate the BPA-specific up-regulations of *in situ* steroidogenesis in other organs, we first examined the changes in *Esrrg* mRNA expression in sex hormone-related organs, such as the cerebellum, heart, kidney, ovary, and testis. At P1, the mRNA expression of *Esr1* in the cerebellum, heart, kidney, and ovary, with the exception of the testis, was up-regulated by both BPA and DES treatment (Figure 7A). However, no significant difference in *Ar* mRNA expression was observed in all organs examined (Figure 7B). In the untreated group, the mRNA expression of *Esrrg* was not detected in the testis at E17 and P1 (Figure 7C). The up-regulation of *Esrrg* mRNA was observed at E17 and restricted to the cerebellum, heart, kidney, and ovary (Figure 7C). The BPA-specific up-regulations of *Cyp19a1*, *Cyp11a1*, and *Nr5a1* mRNA were observed only at P1 in the cerebellum, heart, kidney, and ovary, with the exception of the testis (Figure 8).

DISCUSSION

There has been increasing concern about the effects of EDCs such as BPA on human health [24]. Although the majority of EDCs have the potential to alter the functioning of the reproductive and endocrine system, the actual mechanism responsible for such alterations has not been identified thoroughly. BPA is of concern because its chemical structure resembles that of DES. Several studies have reported that BPA can mimic estrogen action: e.g., induction of vaginal cornification, uterine vascular permeability, growth and differentiation of the mammary gland, and synaptic plasticity in the hippocampus [25] [26] [27] [28]. In the prostate, alterations in normal development can produce permanent changes that persist throughout adulthood and may increase the risk of disease in later life [9]. Thus, our objective was to investigate the biological effects of low-dose BPA on the initial development of primary ducts in the fetal prostate.

During prostatic development, alteration of sex steroid hormone synthesis may be responsible for prostatic anomalies associated with fetal exposure to EDCs. In the present study, we showed that fetal exposure to low-dose BPA increased E₂ levels in P1 UGS of both the male and female, while DES-induced changes were not detected. This alteration was also correlated with increased activity of CYP19A1 (aromatase) in UGS at P1, suggesting the unique action of BPA for *in situ* steroidogenesis in UGS. The BPA-specific increase of E₂ levels in UGS at P1 was correlated with the following: (1) mRNA up-regulations of steroidogenic enzymes such as *Cyp19a1* and *Cyp11a1*; and (2) an increased number of aromatase-expressing mesenchymal cells of UGS (UGM). The enzyme CYP19A1 (aromatase) is responsible for *in situ* E₂ production and the crucial T/E₂ balance necessary for normal embryonic and fetal development, even in males. Our data presented here shows that the up-regulation of *Cyp19a1* mRNA in

BPA-treated UGM was comparable to changes in both *in situ* E₂ production and CYP19A1 (aromatase) activity.

In the present study, we demonstrated that the BPA-specific increase in steroidogenic enzyme mRNA and aromatase-expressing cell number were observed in the mesenchymal component of both the male and female UGS. During embryonic development, the mesenchymal component is involved in the induction and organogenesis of various organs including the prostate, mammary gland, lung, kidney, and pancreas. It has been well established that sub-populations of the mesenchymal component are a source of potent molecules that regulate epithelial growth and differentiation [29]. In the prostate, androgen-responsive signals derived from UGM permissively and instructively induce UGE to form primary ducts of the prostate [30].

Comparison between the neonatal male and female UGS shows a similarity in the condensed mesenchyme of the ventral areas: i.e., the ventral prostate mesenchyme (VPM) in the male and the ventral mesenchymal pad (VMP) in the female [31]. In the male, a defined mesenchyme VPM is specifically associated with ductal branching morphogenesis and cytodifferentiation of the ventral prostate. Females do not usually form a prostate. In a tissue recombination model, the female VMP induces prostate development in response to androgen [32], suggesting that cells within the female VMP have prostatic inductive activity. Moreover, an earlier tissue recombination study showed that the ability of the female UGS to respond to androgens in forming prostate was gradually lost between P1 and P5 [33]. These results suggest strongly that androgen-responsive regulatory molecules are expressed constitutively even in the female VMP. Although the female VMP forms in the absence of androgens, AR expression was observed in the neonatal female VMP in a similar pattern to that observed in the male VPM [34]. Therefore, the BPA-specific increase in E₂ levels might interact with the intracellular AR signaling in both the male VPM and female VMP. However, the morphological changes in neonatal female UGS had not yet been investigated.

Our results suggest that BPA has a stimulatory effect on *in situ* steroidogenesis in P1 UGS of both the male and female at low dose exposure levels. Recently, ESRRG is reported to bind strongly with BPA [35]. Susens *et al.* have reported that expression of ESRRG in the mouse is organ-specific, i.e., ESRRG is expressed in the brain, heart, kidney, and skeletal muscle but not in the lung, spleen, and testis [36]. Our findings showed that the up-regulations of *Cyp19a1* and *Cyp11a1* mRNA by BPA treatment were detected only in organs expressing *Esrrg* mRNA. These data suggest that the possibility of a stimulatory effect on *in situ* steroidogenesis by fetal exposure to low-dose BPA may be a concern not only in UGS, but also in organs expressing ESRRG, such as the brain, heart, kidney, and ovary. It is important to note that Takeda *et al.* have recently reported that ESRRG was detected in the human testis, suggesting that the distribution of ESRRG differs slightly between mice and humans [23].

In the present study, our results showed that the BPA-specific up-regulations of steroidogenic enzyme mRNA in UGS, cerebellum, heart, kidney, and ovary were observed only during the neonatal period (i.e., P0 and P1) but not during the prenatal period (i.e., E17 and E18). During pregnancy in rodents, large amounts of estrogens produced in the maternal ovaries are continuously delivered to the fetus through the placenta. After birth, however, the fetus may be released from the maternal high-estrogen environment. Thus, one possibility is that the maternal high-estrogen environment in pregnancy may protect the fetus from the effect of BPA on *in situ* steroidogenesis during the prenatal period. However, we did not investigate the effects of neonatal BPA treatment on *in situ* steroidogenesis.

The EDCs-induced alterations of the *in situ* estrogen environment depend on each compound. In addition to atrazine and dioxin, the organotin compound tributyltin (TBT) also increases E₂ production in human placental choriocarcinoma cells [37]. TBT has been demonstrated to induce the superimposition of male sex organs, such as a penis and/or a vas deferens, over female sex organs, which is a phenomenon known as imposex [38]. These studies suggest strongly that EDCs might affect fetal development not only by

mimicking the actions of sex steroid hormones but also by alteration of *in situ* steroidogenesis.

In the prostate, AR expressed in mesenchyme is required for directing growth and branching morphogenesis of epithelia, presumably by induction of growth factors [39]. In the present study, we showed that fetal exposure to BPA or DES increased *Ar* mRNA expression in E17 UGM of the male, while *Esr1* mRNA expression was up-regulated in E17 UGM of the female. Recently, Richter *et al.* have reported that *in vitro* BPA treatment stimulates *Ar* and *Esr1* mRNA expression in mesenchymal cells isolated from fetal mouse prostate [40]. Thus, our results support the idea that BPA-induced cell proliferation of the primary prostatic ducts may be caused by inducing *Ar* mRNA expression in the male UGM. In contrast, the induction of *Esr1* mRNA expression by BPA or DES may create a positive feedback loop in the female UGM. In future, further investigation for morphological analysis would be necessary to confirm the effects of up-regulated ESR1 in the female UGS.

In conclusion, we demonstrated the unique action of BPA in the mouse UGS. Specifically, we demonstrated that the increases in E_2 levels and CYP19A1 (aromatase) activity were observed in the BPA-treated UGS but not in the DES-treated UGS. Ricke *et al.* have recently reported that stromal hormone imbalance, a potential source of local E_2 production, may be responsible for prostatic disease such as benign prostatic hyperplasia (BPH) and prostate cancer (PCa) [41]. The data shown in the present study give rise to the concept that the development and differentiation of UGS in mouse fetuses is very sensitive to fetal exposure of low-dose BPA via the mother. Further investigation of various aspects of BPA-specific action is necessary to fully understand the role of BPA as an EDC.

ACKNOWLEDGEMENTS

We thank Prof. Nobuhiro Harada at Department of Biochemistry, Fujita Health University School of Medicine for kindly providing rabbit polyclonal anti-aromatase antibody. We also thank Mrs. Hiroko Nishii for technical support.

REFERENCES

1. Sekizawa J. Low-dose effects of bisphenol A: a serious threat to human health? *J Toxicol Sci* 2008; 33: 389-403.
2. Newbold RR, Jefferson WN, Padilla-Banks E. Prenatal exposure to bisphenol a at environmentally relevant doses adversely affects the murine female reproductive tract later in life. *Environ Health Perspect* 2009; 117: 879-885.
3. McPherson SJ, Ellem SJ, Risbridger GP. Estrogen-regulated development and differentiation of the prostate. *Differentiation* 2008; 76: 660-670.
4. Welshons WV, Nagel SC, vom Saal FS. Large effects from small exposures. III. Endocrine mechanisms mediating effects of bisphenol A at levels of human exposure. *Endocrinology* 2006; 147: S56-69.
5. Schonfelder G, Wittfoht W, Hopp H, Talsness CE, Paul M, Chahoud I. Parent bisphenol A accumulation in the human maternal-fetal-placental unit. *Environ Health Perspect* 2002; 110: A703-707.
6. Tsutsumi O. Assessment of human contamination of estrogenic endocrine-disrupting chemicals and their risk for human reproduction. *J Steroid Biochem Mol Biol* 2005; 93: 325-330.
7. Timms BG, Howdeshell KL, Barton L, Bradley S, Richter CA, vom Saal FS. Estrogenic chemicals in

plastic and oral contraceptives disrupt development of the fetal mouse prostate and urethra. *Proc Natl Acad Sci U S A* 2005; 102: 7014-7019.

8. Ogura Y, Ishii K, Kanda H, Kanai M, Arima K, Wang Y, Sugimura Y. Bisphenol A induces permanent squamous change in mouse prostatic epithelium. *Differentiation* 2007; 75: 745-756.

9. Ho SM, Tang WY, Belmonte de Frausto J, Prins GS. Developmental exposure to estradiol and bisphenol A increases susceptibility to prostate carcinogenesis and epigenetically regulates phosphodiesterase type 4 variant 4. *Cancer Res* 2006; 66: 5624-5632.

10. Markey CM, Luque EH, Munoz De Toro M, Sonnenschein C, Soto AM. In utero exposure to bisphenol A alters the development and tissue organization of the mouse mammary gland. *Biol Reprod* 2001; 65: 1215-1223.

11. Honma S, Suzuki A, Buchanan DL, Katsu Y, Watanabe H, Iguchi T. Low dose effect of in utero exposure to bisphenol A and diethylstilbestrol on female mouse reproduction. *Reprod Toxicol* 2002; 16: 117-122.

12. Kubo K, Arai O, Omura M, Watanabe R, Ogata R, Aou S. Low dose effects of bisphenol A on sexual differentiation of the brain and behavior in rats. *Neurosci Res* 2003; 45: 345-356.

13. Fan W, Yanase T, Morinaga H, Gondo S, Okabe T, Nomura M, Komatsu T, Morohashi K, Hayes TB, Takayanagi R, Nawata H. Atrazine-induced aromatase expression is SF-1 dependent: implications for endocrine disruption in wildlife and reproductive cancers in humans. *Environ Health Perspect* 2007; 115: 720-727.

14. Baba T, Mimura J, Nakamura N, Harada N, Yamamoto M, Morohashi K, Fujii-Kuriyama Y. Intrinsic function of the aryl hydrocarbon (dioxin) receptor as a key factor in female reproduction. *Mol Cell Biol* 2005; 25: 10040-10051.

15. Moustafa GG, Ibrahim ZS, Hashimoto Y, Alkelch AM, Sakamoto KQ, Ishizuka M, Fujita S. Testicular toxicity of profenofos in matured male rats. *Arch Toxicol* 2007; 81: 875-881.

16. Song KH, Lee K, Choi HS. Endocrine disrupter bisphenol a induces orphan nuclear receptor Nur77 gene expression and steroidogenesis in mouse testicular Leydig cells. *Endocrinology* 2002; 143: 2208-2215.

17. Mlynarcikova A, Kolena J, Fickova M, Scsukova S. Alterations in steroid hormone production by porcine ovarian granulosa cells caused by bisphenol A and bisphenol A dimethacrylate. *Mol Cell Endocrinol* 2005; 244: 57-62.

18. Hojo Y, Higo S, Ishii H, Ooishi Y, Mukai H, Murakami G, Kominami T, Kimoto T, Honma S, Poirier D, Kawato S. Comparison between hippocampus-synthesized and circulation-derived sex steroids in the

hippocampus. *Endocrinology* 2009; 150: 5106-5112.

19. Nakanishi T, Nishikawa J, Hiromori Y, Yokoyama H, Koyanagi M, Takasuga S, Ishizaki J, Watanabe M, Isa S, Utoguchi N, Itoh N, Kohno Y, Nishihara T, Tanaka K. Trialkyltin compounds bind retinoid X receptor to alter human placental endocrine functions. *Mol Endocrinol* 2005; 19: 2502-2516.

20. Kanno J, Aisaki K, Igarashi K, Nakatsu N, Ono A, Kodama Y, Nagao T. "Per cell" normalization method for mRNA measurement by quantitative PCR and microarrays. *BMC Genomics* 2006; 7: 64.

21. Ishii K, Imanaka-Yoshida K, Yoshida T, Sugimura Y. Role of stromal tenascin-C in mouse prostatic development and epithelial cell differentiation. *Dev Biol* 2008; 324: 310-319.

22. Jakab RL, Horvath TL, Leranath C, Harada N, Naftolin F. Aromatase immunoreactivity in the rat brain: gonadectomy-sensitive hypothalamic neurons and an unresponsive "limbic ring" of the lateral septum-bed nucleus-amygdala complex. *J Steroid Biochem Mol Biol* 1993; 44: 481-498.

23. Takeda Y, Liu X, Sumiyoshi M, Matsushima A, Shimohigashi M, Shimohigashi Y. Placenta expressing the greatest quantity of bisphenol A receptor ERR{gamma} among the human reproductive tissues: Predominant expression of type-1 ERRgamma isoform. *J Biochem* 2009; 146: 113-122.

24. vom Saal FS, Akingbemi BT, Belcher SM, Birnbaum LS, Crain DA, Eriksen M, Farabollini F, Guillette LJ, Jr., Hauser R, Heindel JJ, Ho SM, Hunt PA, Iguchi T, Jobling S, Kanno J, Keri RA, Knudsen KE, Laufer H, LeBlanc GA, Marcus M, McLachlan JA, Myers JP, Nadal A, Newbold RR, Olea N, Prins GS, Richter CA, Rubin BS, Sonnenschein C, Soto AM, Talsness CE, Vandenberg JG, Vandenberg LN, Walser-Kuntz DR, Watson CS, Welshons WV, Wetherill Y, Zoeller RT. Chapel Hill bisphenol A expert panel consensus statement: integration of mechanisms, effects in animals and potential to impact human health at current levels of exposure. *Reprod Toxicol* 2007; 24: 131-138.

25. Steinmetz R, Mitchner NA, Grant A, Allen DL, Bigsby RM, Ben-Jonathan N. The xenoestrogen bisphenol A induces growth, differentiation, and c-fos gene expression in the female reproductive tract. *Endocrinology* 1998; 139: 2741-2747.

26. Milligan SR, Balasubramanian AV, Kalita JC. Relative potency of xenobiotic estrogens in an acute in vivo mammalian assay. *Environ Health Perspect* 1998; 106: 23-26.

27. Colerangle JB, Roy D. Profound effects of the weak environmental estrogen-like chemical bisphenol A on the growth of the mammary gland of Noble rats. *J Steroid Biochem Mol Biol* 1997; 60: 153-160.

28. Kawato S. Endocrine disrupters as disrupters of brain function: a neurosteroid viewpoint. *Environ Sci* 2004; 11: 1-14.

29. Donjacour AA, Cunha GR. Stromal regulation of epithelial function. *Cancer Treat Res* 1991; 53: 335-364.

30. Hayashi N, Cunha GR, Parker M. Permissive and instructive induction of adult rodent prostatic epithelium by heterotypic urogenital sinus mesenchyme. *Epithelial Cell Biol* 1993; 2: 66-78.
31. Thomson AA. Role of androgens and fibroblast growth factors in prostatic development. *Reproduction* 2001; 121: 187-195.
32. Timms BG, Lee CW, Aumuller G, Seitz J. Instructive induction of prostate growth and differentiation by a defined urogenital sinus mesenchyme. *Microsc Res Tech* 1995; 30: 319-332.
33. Cunha GR. Age-dependent loss of sensitivity of female urogenital sinus to androgenic conditions as a function of the epithelia-stromal interaction in mice. *Endocrinology* 1975; 97: 665-673.
34. Thomson AA, Timms BG, Barton L, Cunha GR, Grace OC. The role of smooth muscle in regulating prostatic induction. *Development* 2002; 129: 1905-1912.
35. Takayanagi S, Tokunaga T, Liu X, Okada H, Matsushima A, Shimohigashi Y. Endocrine disruptor bisphenol A strongly binds to human estrogen-related receptor gamma (ERRgamma) with high constitutive activity. *Toxicol Lett* 2006; 167: 95-105.
36. Susens U, Hermans-Borgmeyer I, Borgmeyer U. Alternative splicing and expression of the mouse estrogen receptor-related receptor gamma. *Biochem Biophys Res Commun* 2000; 267: 532-535.
37. Nakanishi T, Kohroki J, Suzuki S, Ishizaki J, Hiromori Y, Takasuga S, Itoh N, Watanabe Y, Utoguchi N, Tanaka K. Trialkyltin compounds enhance human CG secretion and aromatase activity in human placental choriocarcinoma cells. *J Clin Endocrinol Metab* 2002; 87: 2830-2837.
38. Horiguchi T. Masculinization of female gastropod mollusks induced by organotin compounds, focusing on mechanism of actions of tributyltin and triphenyltin for development of imposex. *Environ Sci* 2006; 13: 77-87.
39. Cunha GR, Donjacour A. Stromal-epithelial interactions in normal and abnormal prostatic development. *Prog Clin Biol Res* 1987; 239: 251-272.
40. Richter CA, Taylor JA, Ruhlen RL, Welshons WV, Vom Saal FS. Estradiol and Bisphenol A stimulate androgen receptor and estrogen receptor gene expression in fetal mouse prostate mesenchyme cells. *Environ Health Perspect* 2007; 115: 902-908.
41. Ricke WA, McPherson SJ, Bianco JJ, Cunha GR, Wang Y, Risbridger GP. Prostatic hormonal carcinogenesis is mediated by in situ estrogen production and estrogen receptor alpha signaling. *FASEB J* 2008; 22: 1512-1520.

FIGURE LEGENDS

Figure 1 BPA-specific increases of E₂ levels and CYP19A1 (aromatase) activity in mouse UGS. E₂ levels (A) and CYP19A1 (aromatase) activity (B) were measured in the untreated control (open bar), BPA-treated (closed bar), and DES-treated (slashed bar) UGS at E17 and P1. *, $p < 0.01$, **, $p < 0.001$ versus control.

Figure 2 BPA-specific up-regulations of steroidogenic enzyme and sex-determining gene mRNA in mouse UGS. The relative mRNA expressions of *Cyp19a1* (A), *Cyp11a1* (B), and *Nr5a1* (C) were determined in the untreated control (open bar), BPA-treated (closed bar), and DES-treated (slashed bar) UGS between E17 and P1. *, $p < 0.05$, **, $p < 0.01$, ***, $p < 0.001$ versus control at each time point. †, $p < 0.01$, ††, $p < 0.001$ versus control at E17.

Figure 3 Restricted BPA-specific up-regulations of steroidogenic enzyme and sex-determining gene mRNA in mesenchymal component of UGS. The relative mRNA expressions of *Cyp19a1* (A), *Cyp11a1* (B), and *Nr5a1* (C) were determined for UGE and UGM of the untreated control (open bar), BPA-treated (closed bar), and DES-treated (slashed bar) UGS at E17 and P1. *, $p < 0.01$, **, $p < 0.001$ versus control.

Figure 4 BPA-specific increases of aromatase-expressing cells in primary cultured UGM. (A-C) Fluorescence signals were detected for the CYP19A1 (aromatase) protein in primary cultured UGM. The nuclei were identified by Ran staining. (D) The number of aromatase-positive cells was counted in primary cultured UGM of the untreated control (open bar), BPA-treated (closed bar), and DES-treated (slashed bar) UGS, and the percentage of aromatase-positive cells was calculated from at least 10 areas. *, $p < 0.01$ versus control. Scale bar = 100 μ m, magnification $\times 400$.

Figure 5 Restricted BPA-specific up-regulation of *Esrrg* mRNA in mesenchymal component of UGS. The relative mRNA expressions of *Esr1* (A), *Ar* (B), and *Esrrg* (C) were determined in UGE and UGM of the untreated control (open bar), BPA-treated (closed bar), and DES-treated (slashed bar) UGS at E17 and P1. *, $p < 0.05$, **, $p < 0.01$, ***, $p < 0.001$ versus control.

Figure 6 BPA-specific increases of ESRRG-expressing cells in primary cultured UGM. (A-C) Fluorescence signals were detected for the ESRRG protein in primary cultured UGM. The nuclei were identified by Ran staining. (D) The number of ESRRG-positive cells was counted in primary cultured UGM of the untreated control (open bar), BPA-treated (closed bar), and DES-treated (slashed bar) UGS, and the percentage of ESRRG-positive cells was calculated from at least 10 areas. *, $p < 0.01$ versus control. Scale bar = 100 μ m, magnification $\times 400$.

Figure 7 BPA-specific up-regulation of *Esrrg* mRNA in sex steroid hormone-related organs. The relative mRNA expressions of *Esr1* (A), *Ar* (B), and *Esrrg* (C) were determined in sex steroid hormone-related organs of the untreated control (open bar), BPA-treated (closed bar), and DES-treated (slashed bar) UGS at E17 and P1. C, cerebellum; H, heart; K, kidney; O, ovary; T, testis. *n.d.*, not detected. *, $p < 0.05$, **, $p < 0.01$, ***, $p < 0.001$ versus control.

Figure 8 BPA-specific up-regulations of steroidogenic enzyme and sex-determining gene mRNA in sex steroid hormone-related organs. The relative mRNA expressions of *Cyp19a1* (A), *Cyp11a1* (B), and *Nr5a1* (C) were determined in sex steroid hormone-related organs of the untreated control (open bar), BPA-treated (closed bar), and DES-treated (slashed bar) UGS at E17 and P1. C, cerebellum; H, heart; K, kidney; O, ovary; T, testis. *, $p < 0.05$, **, $p < 0.01$, ***, $p < 0.001$ versus control.

Table 1 Sequences of oligonucleotide primers used for the real-time PCR analyses

Gene	Primer
<i>Gapdh</i>	F: 5'-AAATGGTGAAGGTCGGTGTG-3' R: 5'-TGAAGGGGTCGTTGATGG-3'
<i>Cyp19a1</i>	F: 5'-GCCCAATGAATTTACCCTCGAA-3' R: 5'-AAGCCAAAAGGCTGAAAGTACCT-3'
<i>Cyp11a1</i>	F: 5'-TCGACTCCTCAGAACTAAGACCTG-3' R: 5'-GTACCCTGGTGTCTTTATAGCCT-3'
<i>Nr5a1</i>	F: 5'-CCTGGGCTGGCTACCTCTATC-3' R: 5'-CGAACTAGAGCCAGAGGAGGAC-3'
<i>Esr1</i>	F: 5'-GCACAGGATGCTAGCCTTGTCTC-3' R: 5'-AATTGTCACCAGCTTGCAGGTTC-3'
<i>Ar</i>	F: 5'-GGCGGTCCTTCACTAATGTCAACT-3' R: 5'-CTGACTTGTGCATGCGGTACTCAT-3'
<i>Esrrg</i>	F: 5'-CCGAGAGTTGGTGGTTATCATTGG-3' R: 5'-GGAAGACCCTCGCCGTGC-3'

Figure 1

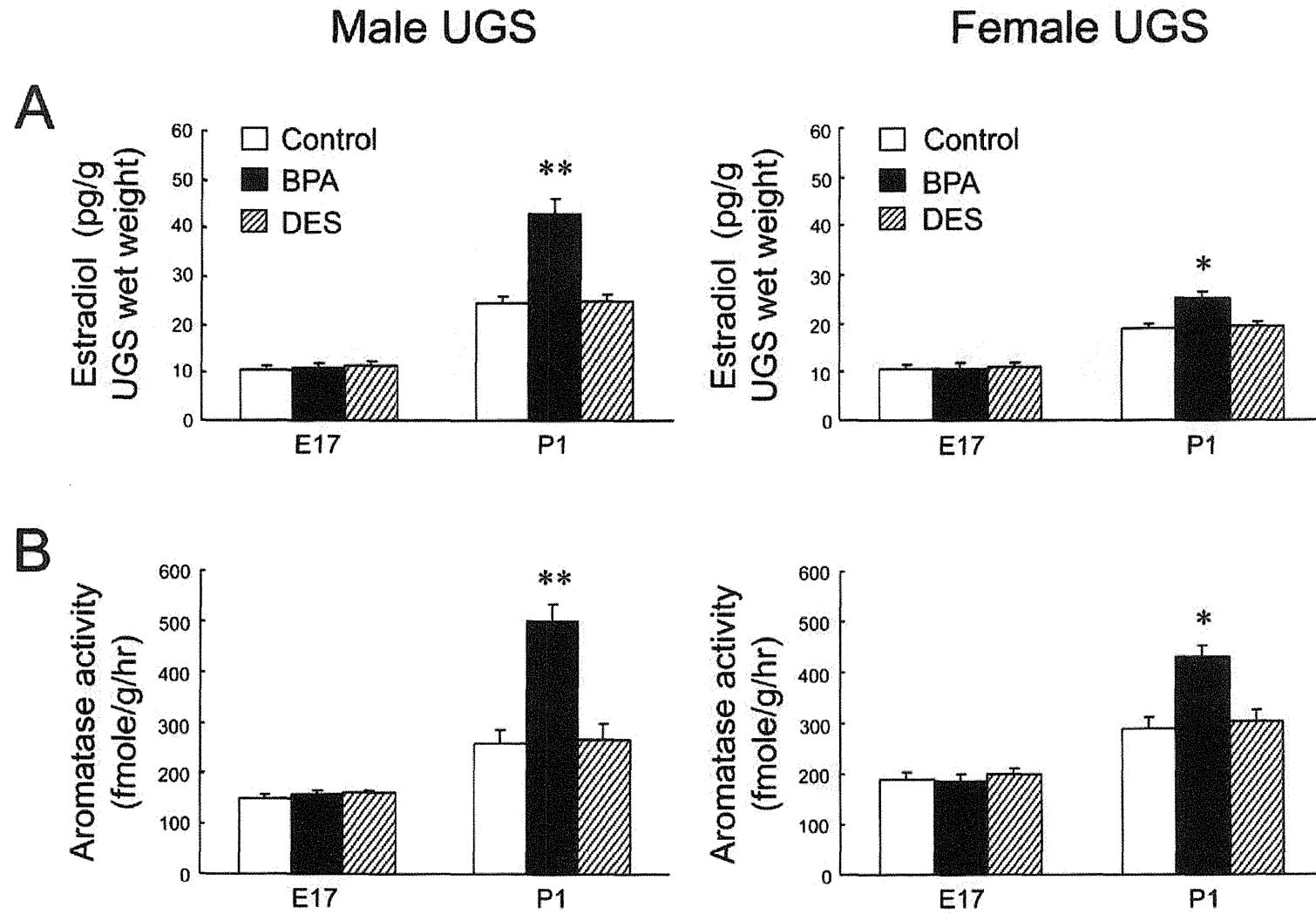


Figure 2

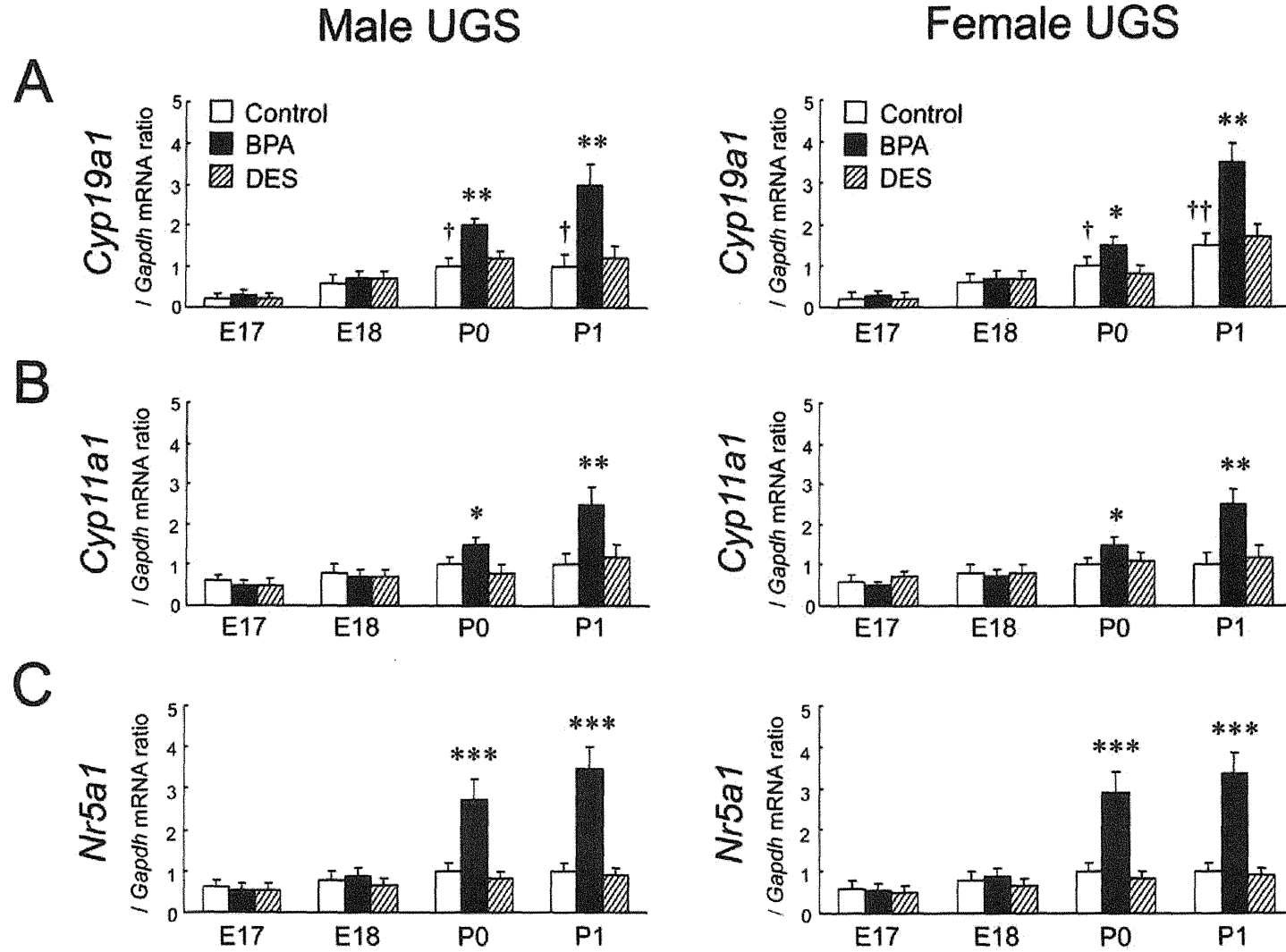


Figure 3

